Journal of Ceramic Processing Research. Vol. 16, Special. 1, pp. 89s~94s (2015)

J O U R N A L O F
Ceramic Processing Research

Experimental study on self-healing effect of FRCC with PVA fibers and additives

Tomoya Nishiwaki*, Haruka Sasaki and Suk-Min Kwon
Department of Architecture and Building Science, Graduate School of Engineering, Tohoku University, Sendai Japan

It has been confirmed that some types of fiber-reinforced cementitious composites (FRCCs), particularly the ones that use synthetic fibers (e.g. polyvinyl alcohol; PVA), have a great capability to self-heal the cracks by some previous research. In this study, self-healing capability of FRCCs with additives such as silica fume and excess PVA dosage was tested. Two experimental studies were carried out to evaluate the self-healing capability with different levels of cracks. As to Test I, freeze/thaw cycles (according to the JIS A 1148 (ASTM C 666-A) method) was subjected to specimens to introduce micro cracks. As to Test II, visible cracks up to 500 μm width were generated by tensile loading test. The damaged FRCC specimens were exposed to several conditions to induce self-healing curing. In the case of Test I (freeze/thaw cycles), the self-healing capability was evaluated by measuring the number of cracks, relative dynamic Young's-modulus (RDYM) and pore structures. In the case of Test II (tensile loading test), the coefficient of watertightness was measured every certain period of time.
Upon exposing to the curing conditions after the damage, the results showed a recovery by means of self-healing effect. In Test I, all of the cracks and RDYM recovered due to the densification of microstructures and filling up of the cracks. In Test II, the recovery of the coefficient of watertightness was confirmed after self-healing curing, which was proportionally consistent during the immersion in water. Moreover, the results showed that an admixture of PVA could be expected to enhance the self-healing capability of cracks without causing any negative impact on the properties of FRCC.

Key words: Self-healing, Fiber reinforced cementitious composite (FRCC), Polyvinyl alcohol (PVA) fiber, PVA additive, Freeze/thaw cycle, Wet/dry cycle.

Introduction

The self-healing concrete has been developed in the hope for "maintenance-free" concrete structures, which is considered to be one of the most promising solutions, especially during the last decade, by a lot of researchers [1-3]. The self-healing approach might be a suitable countermeasure against cracks that inherently occurs in concrete without any human intervention. Such self-healing phenomena can be expected to be more effective in the case of fiber reinforced cementitious composites (FRCC) than in the case of conventional concrete. FRCC has certain mechanical properties that enable the control of crack width propagation in the cement matrix via bridging with randomly distributed short fibers. Since self-healing requires sufficiently small crack widths, FRCCs are expected to demonstrate significant self-healing capability. In previous studies, some types of fiber-reinforced cementitious composites (FRCCs) have been reported to show great capability to self-heal the cracks due to their crack control at sufficiently narrow crack width [4]. FRCC can enhance the autogenous healing effect, which can be seen even in the conventional concrete without special additives/devices. Thus, it might be one of the most promising material for practically realizing self-healing concrete, because no special additives/devices, such as a bacterial approach which is widely spread especially among Europe (e.g., [5]) or embedding some healing agent (adhesives) covered by capsules or vascular approaches (e.g. [6, 7]), are needed. Ubiquitous reinforcing fibers in the cement matrix can enhance the self-healing capability due to crack-width control and acceleration of $CaCO_3$ precipitations [8]. In our previous research [9], we confirmed that FRCC with synthetic fibers offers great potential for the self-healing of cracks. Different types of fibers were concluded to show different levels of self-healing performance. In particular, fibers based on a polar polymer (e.g., polyvinyl alcohol, PVA) promote the precipitation of crystallization products on the crack surface more effectively than other types of fibers do. However, the amount of reinforcing fiber that can be added to FRCC is limited, because large doses of the fiber may cause a decrease in the workability.

In this study, experimental evaluations were carried out using an additional dose of PVA as an admixture with different levels of damage and exposure conditions after inducing damage. In Test I, freeze/thaw cycles test was carried out in order to introduce microcrack damage. To evaluate the self-healing capability of damaged FRCC, the number of cracks, relative dynamic Young's-modulus (RDYM) and mercury intrusion porosimetry (MIP) were measured. In Test II, visible

*Corresponding author:
Tel : +81-22-795-7489
Fax: +81-22-795-4772
E-mail: tomoya.nishiwaki.e8@tohoku.ac.jp

cracks were generated by conducting a tensile loading test. The damaged specimens were exposed to several conditions, i.e. immerse into water and wet/dry cycles. The coefficient of water permeability was measured by conducting a water permeability test, in order to check the effect of self-healing recovery.

Testing Procedures

TEST I (Self-healing after freeze/thaw cycles)

Table 1 shows the mix proportions of the specimens used in Test I. PVA was employed not only as a reinforcing fiber but also as an admixture. PVAs with different degrees of saponification were employed: PVA with a higher degree of saponification (99%) was used as a short reinforcing fiber, and PVA with a lower degree of saponification (96%) was dissolved in the mixing water as an admixture. The latter PVA is soluble in water at room temperature. As a result, the PVA-II series contained a higher total volume content of PVA than did the other series. The dissolved PVA could also serve as a viscous agent to improve the workability and distribution of the reinforcing fibers. On the other hand, lower degrees of saponification could decrease durability because of the relatively high water solubility/absorbency.

The specimens had a prism (40 mm × 40 mm × 160 mm) geometry. Specimens were demolded over 24 hr after casting and they were then cured in a water bath at 20 ºC for up to 10 days. According to the JIS A 1148 "Method of Test for Resistance of Concrete to Freezing and Thawing" (similar to ASTM C 666-A), the specimens were subjected to 300 freeze/thaw cycles. Both freeze and thaw processes occurred under water. The dynamic Young's-modulus was measured every 30 cycles, and RDYM was calculated. After 300 cycles, the specimens were immersed again in water bath at 20 ºC for curing self-healing. Before and after this curing, the number of cracks, RDYM and micro structure were measured by means of the following methods;

Regarding RDYM, the fundamental transverse frequency factor due to longitudinal vibration was measured by Young's modules rigidity meter (MIN-011-0-10, Marui, Japan). It measures the resonance frequency by sweeping the frequency with a computer. Measuring range was from 5,000 Hz from 20,000 Hz. RDYM (%) was calculated by Eq. (1) (according to JIS A 1148)

$$\mathrm{RDYM} = 100 \times (f_n / f_0)^2 \quad (1)$$

Where fn is the fundamental transverse frequency (Hz) after n cycles, and f_0 is the fundamental transverse frequency (Hz) before the freezing thawing test (at 0 cycles).

The number of cracks per unit length was calculated by a method applied by Matsumura *et al* [10]. After cutting the portion of 40mm of the specimen from the end, the cut surface of the test piece was polished by a wet grinding machine (# 700). Then, specimen was washed with distilled water. The black ink was applied to the surface of the specimen after wiping off the surface water. After the black ink completely dried, the specimens were lightly polished again. Then, the cut surface was observed by using a digital microscope (VHX-1000, Keyence, Japan) at 50x magnification. The number of cracks were counted at the across point of each counting lines placed at every 10 mm as shown in Fig. 1. The counted number was divided by the total length of counting line to determine the number of crack per unit length.

Mercury intrusion porosimetry (MIP) (PM60GT-18, Quantachrome Instruments, the US) is used to quantitatively evaluate the microstructures according to JIS R 1655. Two test samples were prepared: one was taken just after freeze/thawing test (up to 300 cycles) and the other was taken after water curing. The samples were cut off from the center of the specimen and were used to measure the pore structure. Before MIP test, the samples were dipped in acetone for 24 hours to prevent any further hydration progress at specific age. Then the samples were dried in an oven at about 105 ºC for 28 hours (i.e. oven dried until constant weight to remove moisture in the pores). The initial

Table 1. Mix proportions (Test I).

Notation	B		W/B	S/B	SP/B	PVA-F (vol.%)	PVA-A (vol.%)
	C	SF					
Control	85	15	0.45	0.45	0.009	–	–
PVA-I						2	1.5
PVA-II							
PVA-III	100	–			0.003		–

[Note] C: High early strength Portland cement (density: 3.14 g/cm^3), SF: Silica fume (density: 2.20 g/cm^3), B: Binder (= C + SF), W: Tap water, S: Silica sand #5 (density: 2.61 g/cm^3, diameter: ~ 500 μm), SP: Super plasticizer (polycarboxylic acid ether system, density: 1.0 g/cm^3), PVA-F: PVA fiber (degree of saponification: 99%, density: 1.30 g/cm^3, diameter: 37 μm, length: 6 mm), PVA-A: PVA admixture (degree of saponification: 96 %, density: 1.30 g/cm^3).

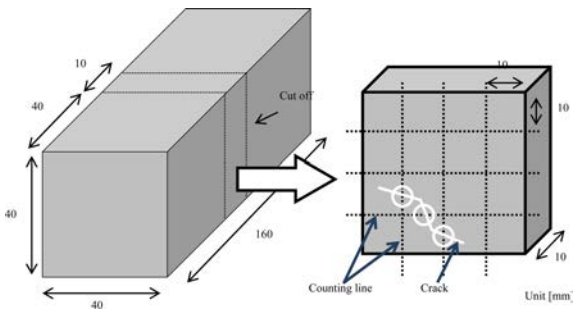

Fig. 1. Counting method of number of cracks.

measurement and the final measurement of the pressure were 140 kPa and 420 MPa, respectively. The velocity of pressure increment was 0.1 MPa/s.

Exposure to several conditions (TEST II)

The employed materials were the same as Test I. Mix proportions were presented in Table 2, PVA-IV series with fly ash was added instead of PVA-III without the additives of pozzolanic material, in order to enhance self-healing capability. In addition, Control (without PVA fiber) series was eliminated because it was not possible to control the crack width during tensile loading. Figure 2 shows an employed specimen, which is a plate of 85 mm × 85 mm × 30 mm and four screw bars (M6) with an anchor nut at the tip. After casting, specimens were settled in a water tank at a temperature of 20 ºC for 7 days. After the first curing step, each specimen was subjected to a uniaxial tension test during which the embedded screw bars generated a crack with a maximum width of approximately 300 μm. The cracked specimens were then subjected to a water permeability test. After the permeability test, the specimens were exposed to different conditions according to Table 3. During the exposure, the water permeability test was carried out again after 3, 14, and 28 days had passed from the start of the exposures, except for Condition 6 (outdoor). During this time, the surface around the cracks was observed by the digital microscope. Figure 3 shows the apparatus of this permeability test (an improvement upon [11]). The coefficient of the water permeability was calculated from the volume of water that permeated the specimen.

In the case of Condition 6, only the PVA-I series specimens were exposed to outdoor condition for 28 days (from 28 November 2013 to 26 December 2013). The average temperature is approximately 5 ºC at Tohoku University in Sendai, Japan. During the exposure period, the water permeability test was again carried out after 3, 9, 21 and 28 days.

Table 2. Mix proportions (Test II).

Notation	B			W/B	S/B	SP/B	PVA-F (vol.%)	PVA-A (vol.%)
	C	SF	FA					
PVA-I	85	15	–	0.45	0.45	0.009	2	–
PVA-II								1.5
PVA-IV	70	–	30					–

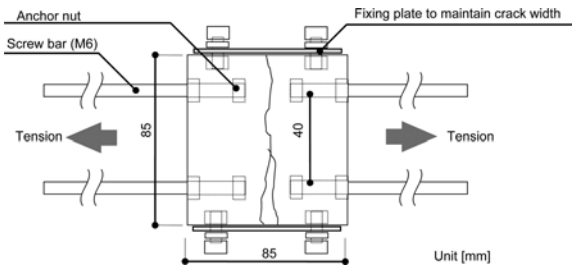

Fig. 2. Employed specimen in Test II.

Table 3. Exposure conditions.

Condition 1	Immersed into water (20 ºC)
Condition 2	Wet in 24 hr and dry in 24 hr (both 20 ºC)
Condition 3	Wet in 24 hr (20 ºC) and dry in 24 hr (40 ºC)
Condition 4	Wet in 6 hr and dry in 42 hr (both 20 ºC)
Condition 5	Wet in 6 hr (20 ºC) and dry in 42 hr (40 ºC)
Condition 6	Exposure to outdoor (5 ºC in average)

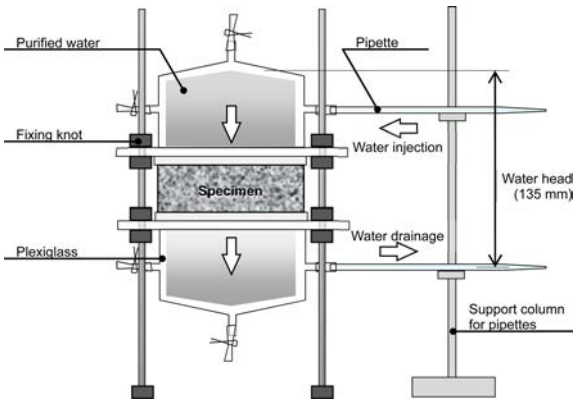

Fig. 3. Apparatus for water permeability test.

Results and Discussion

TEST I

Figure 4 shows the relationship between the number of freeze/thaw cycles and the RDYM. Even after 300 cycles, the RDYM of all the series could be maintained at more than 90%. The PVA-III series without silica fume showed a relatively large degradation. The Control series without PVA fibers also showed continuous degradation of the RDYM. PVA-I and PVA-II showed a similar tendency and maintained a high RDYM of more than 98%. The PVA-II and I series showed a higher freeze-thaw resistance than did the Control series. Moreover, PVA additive with lower degree of saponification did not have any negative effect on the freeze–thaw resistance.

Figure 5 shows the difference in the RDYM values

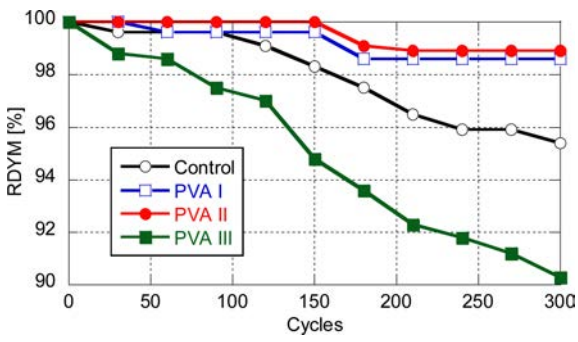

Fig. 4. Relationship between freeze/thaw cycles and RDYM.

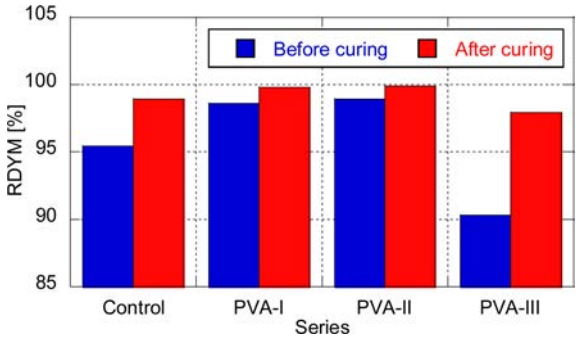

Fig. 5. Comparison of RDYM before and after 28 days of curing.

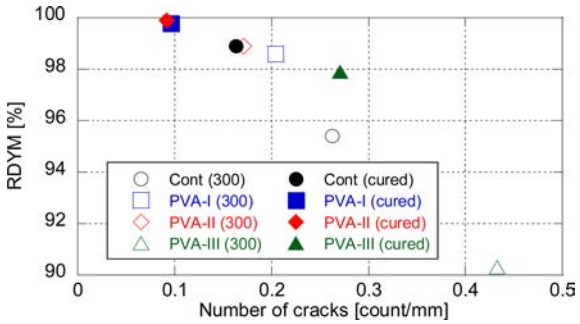

Fig. 6. Relationship between RDYM and number of cracks.

before curing (just after 300 freeze/thaw cycles) and after 28 days of curing in the water bath. The recovery of the RDYM was confirmed in all the series during the curing period. This recovery was led to fill the cracks due to precipitation of $CaCO_3$. In the case of PVA-I and PVA-II, the RDYMs were fully recovered up to 100%. In addition, the pozzolanic reaction of silica fume could enhance the ability to fill up the cracks in all specimens except for the PVA-III series.

The relationship between RDYM and the number of cracks was shown in Fig. 6. In the all series, it was confirmed that the number of cracks of the samples after frost damage decreased after water curing. After the curing, the relationship between the number of cracks and RDYM was maintained in a same proportional shape. Therefore, the occurrence of cracks caused the decline of RDYM. The images of the cracks immediately after the freeze/thaw test and after 28 days of water curing, which were obtained by microscope observation, are shown in Fig. 7. The PVA III series (i.e. without silica fume) showed a large number of cracks immediately after the freeze/thaw test. Comparing the observation of the surface after 28 days of water curing, it was confirmed that number of cracks decreased. On the other hand, the other three series showed few numbers of cracks immediately after the freeze/thaw test, and in case of after 28 days of water curing, these cracks were almost fully closed. From the results mentioned above, the replacement of the silica fume was effective in controlling the cracks from the freeze and thawing test.

Figure 8 shows the cumulative pore volume of all the

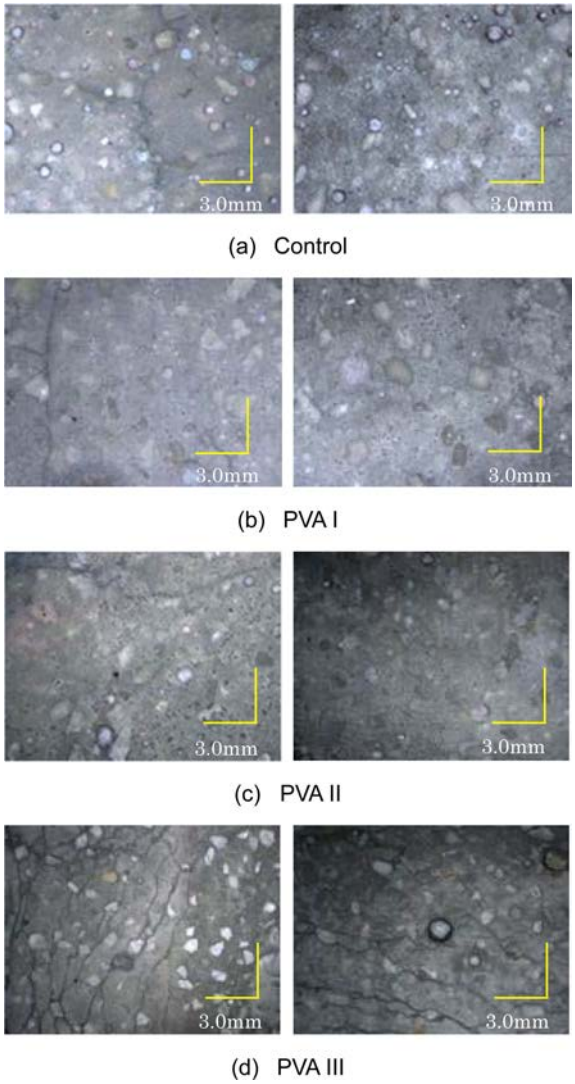

Fig. 7. Microscopic observation of cracks. Before (left) and after (right) 28 day of curing.

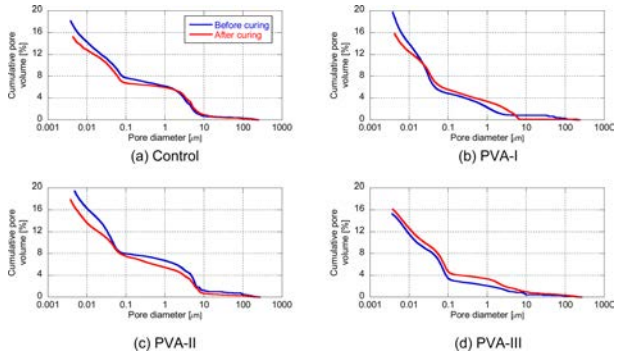

Fig. 8. Pore size distribution before curing (just after 300 freeze/thaw cycles) and after 28 days of curing.

series before and after 28 days of water curing, in terms of the relationship between the pore diameter and the cumulative pore volume. Figure 9 shows the difference in the cumulative pore volume before curing (damaged by freeze/thaw cycles) and after 28 days of curing. According to Fig. 9, in the case of the PVA-II

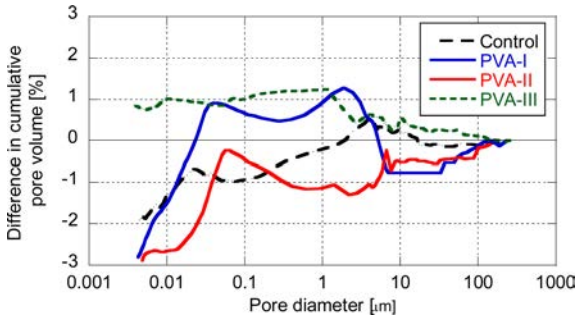

Fig. 9. Difference of cumulative pore volume between before and after curing.

series with both PVA fiber and additive, the cumulative pore volume decreased for all range of pore size, and the difference was the largest among the other series. The PVA-I series also showed a decrease in the cumulative pore volume; however, no densification of pore structure was confirmed over the range 0.1 μm to 1 μm. This result demonstrates that the use of PVA as an additive could enhance the precipitation of $CaCO_3$ not only around the bridging fibers, but also at the surface of the cracks. The Control series without PVA fiber also showed a decreasing trend in the cumulative pore volume. In the case of PVA-III without silica fume, the cumulative pore volume increased, but the pore distribution slightly changed. Edvardsen reported that the chemical products formed in the pozzolanic reaction of silica fume can fill micropores with the size ranging from 0.005 μm to 1 μm [12]. The results for all the samples except PVA-III without silica fume agreed with the aforementioned trend, thus indicating that silica fume contributes to the densification of the microstructures.

TEST II

Figure 10 shows the relationship between the number of cycles and normalized water permeability coefficient. Forty-eight hours were converted as 1 cycle. In the case of Condition 1 with the all series, the highest recovery ratio was obtained. In particular, PVA-II series with PVA additive showed the highest value of recovery ratio among three series, not only in Condition 1 but also the other Conditions mentioned below. That is, PVA additive could enhance the capability of self-healing effect. For Conditions 2 and 4 with the same moderate temperature (20 °C), Condition 2 with longer immersion time showed better recovery than Condition 4 with the all three series. That is, the coefficient of water permeability can decrease with longer immersing time in water. On the other hand, in case of severer dry atmosphere (40 °C) in Conditions 3 and 5, a smaller recovery ratio was obtained. Figure 11 shows the relationship between actual immersing time in water and normalized water permeability coefficient. This graph shows that the recovery ratio in Conditions 2 and 4 with the same temperature was almost as the same as the tendency of Condition 1. On the other hand, Conditions 3 and 5 that were exposed to an intensively dry condition (40 °C) showed a small recovery rate. In other words, the water permeability coefficient was proportionally recovered with the wet curing time if it was not located at the same temperature condition.

Figure 12 shows the relationship between exposure time and coefficient of water permeability in Condition 6, which considers the amount of rainfall during the exposure period. According to this graph, the reduction in the coefficient of water permeability was confirmed

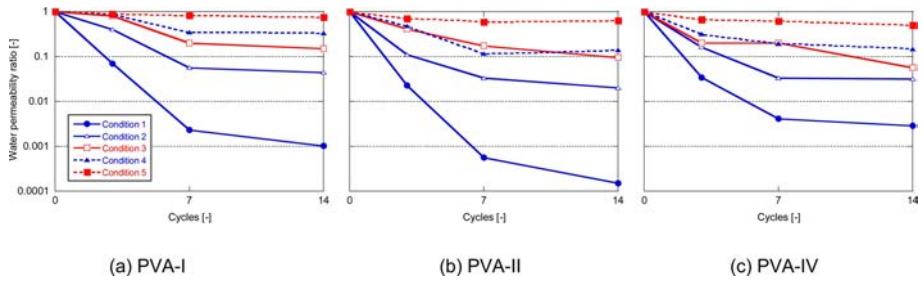

Fig. 10. Relationship between recovery ratio and curing cycles.

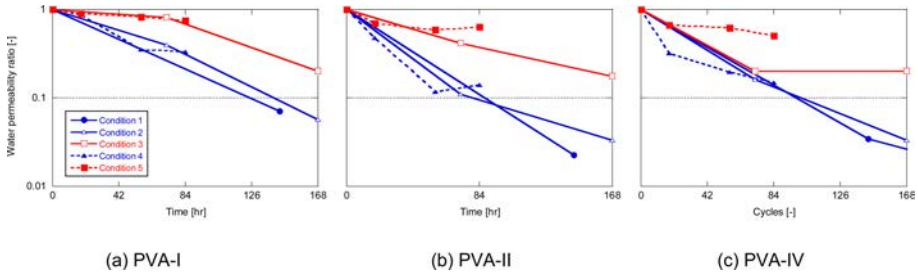

Fig. 11. Relationship between recovery ratio and time to immerse into water.

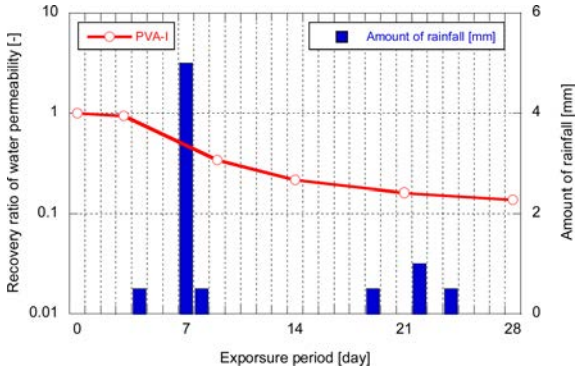

Fig. 12. Recovery ratio and amount of rainfall during the exposure period.

between the 3rd and the 9th day after the start of exposure when rainfall occurred. Filling of cracks and resulting recovery of watertightness due to water supply by rainfall were confirmed. These results agree with the results of Conditions 2 to 5, in which the recovery of watertightness depended on the wetting time in dry/wet cycle tests (Fig. 11). This means that the specimens show self-healing capability upon discontinuous supply of water during rainfall when watertightness is required.

Conclusions

In this study, experimental studies were carried out to evaluate the self-healing capability of FRCCs with additives, i.e., silica fume and excess PVA. The following conclusions could be drawn from the experimental results:

FRCC with both PVA fiber and silica fume showed a high freeze-thaw resistance. PVA additive with lower degree of saponification did not have any negative effect on the freeze–thaw resistance.

The RDYM of FRCCs degraded because of the freeze/thaw cycles but was recovered by the self-healing effect during water curing. The pozzolanic reaction of silica fume could help accelerate the filling up of cracks and pores.

According to the results of MIP measurements, the cumulative pore volume decreased in the case of FRCCs with silica fume. Moreover, the combination of silica fume and PVA fiber and/or additive was preferable for enhancing the self-healing effect.

The watertightness recovery by means of self-healing during wet/dry cycles was confirmed to be strongly affected by the wetting time. In particular, it was confirmed that self-healing performance proportionally increased as the wetting time for Conditions 2 and 4 increased in this study.

In case of PVA-II series with PVA additive, the highest ratio of recovery was obtained during wet/dry cycles.

In outdoor exposure test, the progress of self-healing was confirmed to be relevant to the rainfall within the exposure period.

Acknowlegdments

This work was partially supported by JSPS KAKENHI Grant Number #23686078 and #26289186.

References

1. H. Mihashi, and T. Nishiwaki, “Development of Engineered Self-Healing and Self-Repairing Concrete-State-of-the-Art Report,” *Journal of Advanced Concrete Technology,* vol. 10, no. 5, pp. 170-184, 2012.
2. M. De Rooij, K. Van Tittelboom, N. De Belie, and E. e. Schlangen, *Self-Healing Phenomena in Cement-Based Materials-State-of-the-Art Report of RILEM Thechnical Committee 221-SHC*: *Self-Healing Phenomena in Cement-Based Materials*: Springer, 2013.
3. S. Igarashi, M. Kunieda, and T. Nishiwaki, “Research activity of JCI technical committee TC-075B: Autogenous healing in cementitious materials.” pp. 89-96.
4. E. Herbert, and V. Li, “Self-Healing of Microcracks in Engineered Cementitious Composites (ECC) Under a Natural Environment,” *Materials,* vol. 6, no. 7, pp. 2831-2845, 2013.
5. H. M. Jonkers, “Self Healing Concrete: A Biological Approach,” *Self Healing Materials. An Alternative Approach to 20 Centuries of Material Science*, S. van der Zwaag, ed., pp. 195-204: Springer, 2007.
6. T. Nishiwaki, H. Mihashi, B.-K. Jang, and K. Miura, “Development of Self-Healing System for Concrete with Selective Heating around Crack,” *Journal of Advanced Concrete Technology,* vol. 4, no. 2, pp. 267-275, 2006.
7. C. Joseph, R. Lark, B. Isaacs, D. Gardner, and A. D. Jefferson, “Experimental investigation of adhesive-based self-healing of cementitious materials,” *Magazine of Concrete Research,* vol. 62, no. 11, pp. 831-843, 2010.
8. D. Homma, H. Mihashi, and T. Nishiwaki, “Self-Healing Capability of Fibre Reinforced Cementitious Composites,” *Journal of Advanced Concrete Technology,* vol. 7, no. 2, pp. 217-228, 2009.
9. T. Nishiwaki, M. Koda, M. Yamada, H. Mihashi, and T. Kikuta, “Experimental Study on Self-Healing Capability of FRCC Using Different Types of Synthetic Fibers,” *Journal of Advanced Concrete Technology,* vol. 10, no. 6, pp. 195-206, 2012.
10. T. Matsumura, O. Katsura, and T. Yoshino, “Properties of frost damaged concrete and the estimation of the degree of frost damage,” *Journal of Structural and Construction Engineering* (*Transactions of AIJ),* vol. 563, pp. 9-13, 2003. (in Japanese).
11. Y. Kishimoto, S. Hokoi, K. Harada, and S. Takada, “The Effect of Vertical Distribution of Water Permeability on the Modeled Neutralization Process in Concrete Walls,” *Journal of ASTM International,* vol. 4, no. 1, pp. JAI100323, 2007.
12. C. Edvardsen, “Water permeability and autogenous healing of cracks in concrete,” *ACI Materials Journal,* vol. 96, pp. 448-454, 1999.